Quasi-Unsupervised Learning of Open Circuit Voltage Profiles for Efficiency Degradation Diagnosis in Operation

Masahito Arima[1*], Lei Lin[1], and Masahiro Fukui[2]
[1] Daiwa Can Company, Kanagawa, Japan.
[2] Ritsumeikan University, Shiga, Japan.
m-arima@mail.daiwa-can.co.jp, mfukui@fc.ritsumei.ac.jp

Abstract

The main focus of LIB degradation has been capacity fade so far. On the other hands, efficiency degradation was pointed out in recent years. Battery aggregation, that is expected to absorb the surplus of variable renewable energies like photovoltaic energy, would be affected in terms of economic gain decrease by efficiency degradation. Reuse LIB would be used as a component of aggregation in the future, naturally, the variety of charge–discharge efficiency might be more complex. To improve an operation efficiency of aggregation including reuse LIB, we proposed the quasi-unsupervised learning of open circuit voltage profiles. This method showed good accuracy of the estimation of charge–discharge energy. From this, it is expected that this diagnosis could be contribute to an economic improvement of battery aggregation.

1 Introduction

1.1 Variable Renewable Energies and Battery Aggregation

The variable renewable energies like photovoltaic and wind energy have been increasing (IRENA, 2021), consequently, the problems of surplus electric energy are occurred. One of well-known problems is ‘Duck Curve’ (CAISO, 2016). This is the substantial demand profile with a characteristic shape like duck. That is to say, the abdominal region bulge is shaped by a mass generation of photovoltaic energy. It indicates an over-generation risk by transcending abilities of thermal power generation control and demand generation. As a matter of fact, a large-scale reductive control of variable renewable energies has been occurred in Kyushu, Japan (Kyushu Electric Power

[*] Created this document

Transmission and Distribution Co., 2021). Naturally, it would be resulted in the loss of economic and environmental benefits despite of renewable energy capital investment.

One of its expected solutions is aggregated rechargeable batteries supported by IoT(Isono *et al.*, 2013). That is, the surplus renewable energy could be charged, and discharged later in the time of demand dominance. Lithium-ion battery (LIB) is an important candidate and has been adopted as the components of electric vehicles and stable energy storage systems. For lower resource demands, lower prices and more commercially widespread of LIB, many considerations of reuse (Ahmadi *et al.*, 2017) have been carried out. In consequence, new international standard of requirements for reuse of LIB are under discussion as IEC 63330 aiming for issuance at the end of 2023. From this, we can understand that a lot of aggregated rechargeable batteries consisted of reuse LIB would be popular in the future.

1.2 Research Question

LIB has an important characteristic of performance decline depending on cycle times and storing period (Ramadass *et al.*, 2002) (Schmitt *et al.*, 2017) (Farmann and Sauer, 2017). It is called degradation. A decrease of full-charge capacity is discussed as a main aspect of the degradation. Therefore, a lot of capacity degradation diagnosis of LIB have been studied (Hou *et al.*, 2020). On the other hands, a decrease of charge–discharge energy efficiency called 'efficiency degradation' was reported as another aspect of degradation in recent years (Redondo-Iglesias, Venet and Pelissier, 2019). It causes the increase of energy loss during LIB operation (Arima *et al.*, 2018). Especially, it would induce the order effect of charging in the case of aggregated multiple LIBs (Arima, Lin and Fukui, 2019a). This can be understood in the following way. A degradation degree of each LIB differs since it depends on the conditions of operation. In addition, aggregated batteries could include various LIB of models, manufacturers, and reuse histories. This naturally indicates that each LIB has various characteristic of charge–discharge efficiency. Operation of high efficiency LIB could be resulted in low losses of energy and economic gain. How to find a highly efficient LIB would be necessary for economic and energy saving operation of battery aggregation. Namely, an efficiency degradation diagnosis is necessary instead of capacity.

An efficiency degradation diagnosis has three essential parameters. That is, a value of full charge capacity, and profiles of open circuit voltage and internal impedance (Arima, Lin and Fukui, 2019b). A lot of cases of degradation diagnosis of full charge capacity were already reported as mentioned above. Internal impedance could be estimated by regressive algorithms like Kalman filter (Plett, 2004). However, a profile of open circuit voltage is usually given as a premise in the case of Kalman filter. It is difficult to estimate profiles of open circuit voltage while keeping estimation accuracies of state of charge that is main purpose (Haus and Mercorelli, 2020). Especially, the estimation of transitive profiles of open circuit voltage depending on degradation by this have not been reported. Therefore, the estimation of profiles of open circuit voltage is important for an efficiency degradation diagnosis.

Moreover, it is desirable that the training data of efficiency degradation diagnosis is few. In this case, the measurement data of charge–discharge cycle test for establishing LIB's degradation models is applicable. A large amount of training data would improve the accuracy of these models however it would be necessary to spend many times and works of measurements. Furthermore, there would be many models and manufacturers of aggregated LIB, therefore there would be a lot of test samples to be measured.

In consequence, the estimation of open circuit voltage profiles with few teacher data, that is, quasi-unsupervised learning, is required. In addition, it should be carried out using data measured by a battery management system mounted on LIB for reducing its cost.

1.3 Proposal

There are many reports of open circuit voltage profile measurements, and these could be roughly divided into two groups. One group is 'pseudo open circuit voltage (pOCV)' (Pastor-Fernández *et al.*, 2019). pOCV is the method of charge–discharge in the range of full-discharge to full-charge with lower than 10 hours rate constant current (C/10). Other is called 'Galvanostatic intermittent titration technique (GITT)' (Birkl *et al.*, 2015). GITT is the method of square waved current charge or discharge with long time relaxation between waves. The conditions of pOCV and GITT are quite different from battery aggregation. We propose the unsupervised learning of open circuit voltage profiles using data of a battery management system. The contribution of this study is the adaption to real LIB operation of profile information acquisition.

2 Proposed Method

The unsupervised learning of open circuit voltage profiles that we proposed is described as below.

2.1 Deformative Learning of Open Circuit Voltage Profiles

This method adopts the additive processing of gaussian function profiles estimated by the value of open circuit voltage at that time. The equation of it is defined as follows.

$$\boldsymbol{\hat{V}_{oc-c} = \hat{V}_{oc} + M = \begin{pmatrix} \hat{V}_{oc,1} \\ \hat{V}_{oc,2} \\ \vdots \\ \hat{V}_{oc,99} \end{pmatrix} + \begin{pmatrix} M_1 \\ M_2 \\ \vdots \\ M_{99} \end{pmatrix}}$$

$$\boldsymbol{M_l = \tilde{V}_{oc} L exp\left(-\frac{\left(10^{-2} l - S_{oc,0}\right)^2}{2\sigma^2}\right)}$$

$$\boldsymbol{1 \leq l \leq 99, l \in R^+} \tag{1}$$

Where $\hat{V}_{oc-c}$ denotes the estimated open circuit voltage profile after transformation, $\hat{V}_{oc}$ is the pre-estimated open circuit voltage profile and $\hat{V}_{oc,l}$ are the sample values of $\hat{V}_{oc}$ for each 0.01 state of charge, M is the deformation amount and M_l are the sample values of M for each 0.01 state of charge, $\tilde{V}_{oc}$ is the calculated estimation error of open circuit voltage, L is the learning rate, σ is a standard deviation of gaussian function namely the index of deformation width, $S_{oc,0}$ is the deformation center on the axis of state of charge S_{oc}. The image of one deformation process is described in Fig.1.

$\tilde{V}_{oc}$ was calculated from chronological data of charge–discharge cycles. Charge–discharge voltage $V_{c,d}$ can be defined as follows.

$$\boldsymbol{V_{c,d} = \left(\hat{V}_{oc} + \tilde{V}_{oc}\right) + \left(\hat{R} + \tilde{R}\right) I_{c,d}} \tag{2}$$

Where $\hat{R}$ denotes the estimated internal resistance and $\tilde{R}$ is the estimation error of it, $I_{c,d}$ is the charge–discharge current and it defined charge as positive value and discharge as negative. In this study, it was assumed that $\hat{R}$ is given as the correct values from calculation of chronological data, and the contributions of errors of open circuit voltage and internal resistance are equal, that can be given as follows.

$$\frac{1}{2}\left(V_{c,d} - \hat{V}_{c,d}\right) = \tilde{V}_{oc} = \tilde{R}I_{c,d} \tag{3}$$

$\tilde{V}_{oc}$ was calculated by comparing measured charge–discharge voltage with $\hat{V}_{oc}$ and contributions of errors according to equation (2) and (3). Thereafter, $\hat{V}_{oc-c}$ was calculated based on the additive gaussian sample values M adjusted by learning rate L. $\hat{V}_{oc}$ would be corrected without training data by repeating a series of learning calculation periodically during charge–discharge cycles. It should be noted that the first $\hat{V}_{oc}$ values must be given artificially. Namely, it can be said as quasi-unsupervised learning.

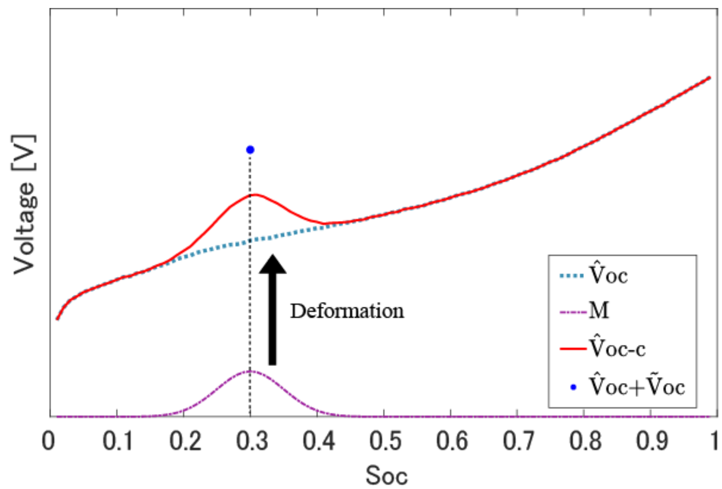

Figure 1: The image of one deformation process of open circuit voltage profile learning.

2.2 Calculation of Charge–Discharge Energy

In this study, the equation of open circuit voltage profile was defined as follows (Plett, 2004).

$$V_{oc}(S_{oc}) = K_1 + \frac{K_2}{S_{oc}} + K_3 S_{oc} + K_4 \ln(S_{oc}) + K_5 \ln(1 - S_{oc}) \tag{4}$$

In this equation, the profile was denoted as a function of S_{oc}. $V_{oc}(S_{oc})$ was fitted by the estimated sample values $\hat{V}_{oc-c}$ based on the deformative learning of equation (1)-(3). That is, $\hat{V}_{oc}$ can be denoted as the sample values based on equation (4) as follows.

$$\hat{V}_{oc} = \begin{bmatrix} K_1 \\ K_2 \\ \vdots \\ K_5 \end{bmatrix}^{\mathsf{T}} \begin{bmatrix} S_1^{5\times1} \; S_2^{5\times1} \; \cdots \; S_{99}^{5\times1} \end{bmatrix} = \begin{bmatrix} \hat{V}_{oc,1} \\ \hat{V}_{oc,2} \\ \vdots \\ \hat{V}_{oc,99} \end{bmatrix}$$

$$S_l^{5\times 1} = \begin{bmatrix} \mathbf{1} \\ \mathbf{10^2 l^{-1}} \\ \mathbf{10^{-2} l} \\ \mathbf{\ln(10^{-2} l)} \\ \mathbf{\ln(1 - 10^{-2} l)} \end{bmatrix} \tag{5}$$

$S_l^{5\times 1}$ are coefficient vector of equation (4). Updated $V_{oc}(S_{oc})$ were fitted based on the evaluation function J_1 including calculation of error with $\hat{V}_{oc-c}$ as follows.

$$\boldsymbol{J_1} = \left\| \begin{bmatrix} \boldsymbol{K_1} \\ \boldsymbol{K_2} \\ \vdots \\ \boldsymbol{K_5} \end{bmatrix} \left[\boldsymbol{S_1^{5\times 1}}\ \boldsymbol{S_2^{5\times 1}}\ \cdots\ \boldsymbol{S_{99}^{5\times 1}} \right] - \boldsymbol{\hat{V}_{oc-c}} \right\| \tag{6}$$

The estimated sampling data of internal resistance $\hat{R}$ was fitted as 6th order polynomial of S_{oc} as follows.

$$\boldsymbol{R(S_{oc})} = \sum_{i=0}^{6} \boldsymbol{K_{i+6} S_{oc}}^{i} \tag{7}$$

based on correct values calculated from chronological charge–discharge data as follows.

$$\boldsymbol{J_2} = \left\| \begin{bmatrix} \boldsymbol{K_6} \\ \boldsymbol{K_7} \\ \vdots \\ \boldsymbol{K_{12}} \end{bmatrix} \left[\boldsymbol{T_1^{7\times 1}}\ \boldsymbol{T_2^{7\times 1}}\ \cdots\ \boldsymbol{T_{99}^{7\times 1}} \right] - \boldsymbol{\hat{R}} \right\|$$

$$\boldsymbol{T_l^{7\times 1}} = \begin{bmatrix} (\mathbf{10^{-2}} \boldsymbol{l})^{\mathbf{0}} \\ (\mathbf{10^{-2}} \boldsymbol{l})^{\mathbf{1}} \\ \vdots \\ (\mathbf{10^{-2}} \boldsymbol{l})^{\mathbf{6}} \end{bmatrix} \tag{8}$$

$T_l^{7\times 1}$ are coefficient vector of equation (7) and $R(S_{oc})$ were fitted based on the evaluation function J_2.

The values of full charge capacity C_{fc} were set as a measured and calculated values of charge–discharge of each cycle. Calculation of charge–discharge energy $W_{c,d}$ was carried out as follows.

$$\boldsymbol{W_{c,d}} = \boldsymbol{C_{fc}} \int \boldsymbol{V_{oc}(S_{oc})} + \boldsymbol{I_{c,d}(S_{oc}) R(S_{oc})}\, \boldsymbol{dS_{oc}} \tag{9}$$

$I_{c,d}(S_{oc})$ is the function of operation current and it was defined by the charge-discharge operator. Calculation of equation (9) was practically carried out as sectional quadrature. The estimation of charge and discharge energy each would result in that of energy efficiency, namely, it could be said as efficiency degradation.

3 Verification

For the verification of this profile learning, offset and noise were added to some parameters. First, +10 % offset error was added to the overall profile of open circuit voltage which was set prior to all learning processes. This was the assumption of reuse LIB having unknown profiles that was introduced in a battery aggregation. Second, maximum ±25 % gaussian noise was added to an internal resistance value of each learning opportunity. This was the assumption of estimation error by Kalman filter or another similar method. In this verification, the learning rate L was set as 3 types of fast, medium, and slow. In addition, the index of deformation width σ was adjusted depending on L.the detailed learning conditions are shown in Table 1.

This verification was carried out based on the chronological data of 700 times charge–discharge cycle of LIB module. The detailed cycle conditions are shown in Table 2. The results were shown in Fig 2. Black lines are actual values of each cycle charge–discharge energy. And red, blue, and green lines are the estimated one based on the deformative learning of open circuit voltage. Solid lines are denoted as charge, and dot lines are denoted as discharge. In the case of condition A, the estimated values were fitted to the actual values within only dozens of cycles. On the other hands, about 150 cycles were necessary in condition B, and about 500 cycles in condition C. The errors of condition A in the range between 601 to 700 cycles were less than 0.3 % in charge, and 0.7 % in discharge. From this, we can conclude in the following way. This proposed method of quasi-unsupervised learning of open circuit voltage profiles could realize the efficiency degradation diagnosis of LIB in combination with capacity degradation diagnosis and internal resistance estimation. Together with this, it is important that the appropriate values of L and σ are selected. We should note that it could be valid for reuse LIB having unknown profiles.

Condition	L	σ
A (fast)	1.374×10^{-1}	1.300×10^{-2}
B (medium)	2.600×10^{-3}	4.250×10^{-2}
C (slow)	1.610×10^{-5}	2.062×10^{-1}

Table 1: The conditions of deformative learning of open circuit voltage.

Sample details	8 series LIB module (NiMnCo cathode and C anode)
Typical characteristics	29.6 V, 50 Ah, 1.48 kWh
Input and output power	1085 W (constant power)
Range of state of charge	0 to 1
Temperature of cycle test chamber	Room temperature

Table 2: The conditions of charge–discharge cycle test of LIB module.

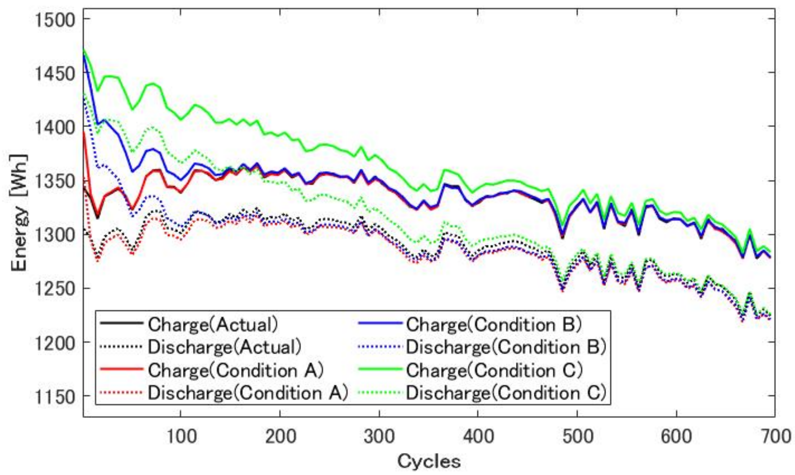

Figure 2: The image of one deformation process of open circuit voltage profile learning.

4 Conclusion

In this study, we pointed out the problem of upcoming reuse LIBs from the point of efficiency degradation. From this, we proposed the quasi-unsupervised learning of open circuit voltage profiles. Compared to pOCV or GITT, this method has a demerit that an open circuit voltage profile might not be obtained from only one charge–discharge process. On the other hands, the merit is a high practicality based on the adaptability of real LIB operation. Therefore, it could realize the efficiency degradation diagnosis in combination of capacity and internal resistance estimation. Moreover, wide variety of open circuit voltage profiles would be expressed by not only reuse but also the difference of active materials like iron phosphate cathode and titanium oxide anode, and the proposed method might be applicable these overall conditions. It is expected that this diagnosis could be contribute to an economic improvement of battery aggregation.

References

Ahmadi, L. *et al.* (2017) ‘A cascaded life cycle: reuse of electric vehicle lithium-ion battery packs in energy storage systems’, *The International Journal of Life Cycle Assessment*, 22(1), pp. 111–124. doi: 10.1007/s11367-015-0959-7.

Arima, M. *et al.* (2018) ‘An Examination about Economic Efficiency Estimation Model of Lithium-ion Batteries’, *Journal of Japan Society of Energy and Resources*, 39(3), pp. 11–20.

Arima, M., Lin, L. and Fukui, M. (2019a) ‘Case study of photovoltaic energy surplus absorption by charging lithium-ion batteries considering charge-discharge energy efficiency’, in *ICCE-Berlin, IEEE International Conference on Consumer Electronics - Berlin*. doi: 10.1109/ICCE-Berlin47944.2019.8966214.

Arima, M., Lin, L. and Fukui, M. (2019b) ‘Three degradation parameters estimation of a LIB module using single indicator for in-situ charge-discharge energy prediction’, in *INTELEC, International Telecommunications Energy Conference (Proceedings)*. doi: 10.1109/INTLEC.2018.8612409.

Birkl, C. R. *et al.* (2015) ‘A Parametric Open Circuit Voltage Model for Lithium Ion Batteries’, *Journal of The Electrochemical Society*, 162(12), pp. A2271–A2280. doi: 10.1149/2.0331512jes.

CAISO (2016) *What the duck curve tells us about managing a green grid*. Available at: https://www.caiso.com/documents/flexibleresourceshelprenewables_fastfacts.pdf (Accessed: 1 June 2021).

Farmann, A. and Sauer, D. U. (2017) ‘A study on the dependency of the open-circuit voltage on temperature and actual aging state of lithium-ion batteries’, *Journal of Power Sources*, 347, pp. 1–13. doi: 10.1016/j.jpowsour.2017.01.098.

Haus, B. and Mercorelli, P. (2020) ‘Polynomial Augmented Extended Kalman Filter to Estimate the State of Charge of Lithium-Ion Batteries’, *IEEE Transactions on Vehicular Technology*, 69(2), pp. 1452–1463. doi: 10.1109/TVT.2019.2959720.

Hou, Q. *et al.* (2020) ‘Embedding scrapping criterion and degradation model in optimal operation of peak-shaving lithium-ion battery energy storage’, *Applied Energy*, 278, p. 115601. doi: 10.1016/j.apenergy.2020.115601.

IRENA (2021) *Renewable Capacity Statistics 2021*. Available at: https://www.irena.org/publications/2021/March/Renewable-Capacity-Statistics-2021 (Accessed: 1 January 2021).

Isono, E. *et al.* (2013) ‘Development of battery aggregation technology for smart grid’, in *2013 IEEE Grenoble Conference*. IEEE, pp. 1–6. doi: 10.1109/PTC.2013.6652141.

Kyushu Electric Power Transmission and Distribution Co., I. (2021) *Area supply and demand results*. Available at: https://www.kyuden.co.jp/td_service_wheeling_rule-document_disclosure (Accessed: 1 June 2021).

Pastor-Fernández, C. *et al.* (2019) ‘Critical review of non-invasive diagnosis techniques for quantification of degradation modes in lithium-ion batteries’, *Renewable and Sustainable Energy Reviews*, 109, pp. 138–159. doi: 10.1016/j.rser.2019.03.060.

Plett, G. L. (2004) ‘Extended Kalman filtering for battery management systems of LiPB-based HEV battery packs: part 2. Modeling and identification’, *Journal of Power Sources*, 134(2), pp. 262–276. doi: 10.1016/j.jpowsour.2004.02.032.

Ramadass, P. *et al.* (2002) ‘Capacity fade of Sony 18650 cells cycled at elevated temperatures’, *Journal of Power Sources*, 112(2), pp. 606–613. doi: 10.1016/S0378-7753(02)00474-3.

Redondo-Iglesias, E., Venet, P. and Pelissier, S. (2019) ‘Efficiency Degradation Model of Lithium-Ion Batteries for Electric Vehicles’, *IEEE Transactions on Industry Applications*, 55(2), pp. 1932–1940. doi: 10.1109/TIA.2018.2877166.

Schmitt, J. *et al.* (2017) ‘Impedance change and capacity fade of lithium nickel manganese cobalt oxide-based batteries during calendar aging’, *Journal of Power Sources*, 353, pp. 183–194. doi: 10.1016/j.jpowsour.2017.03.090.